Materials Letters 180 (2016) 77–80

Contents lists available at ScienceDirect

Materials Letters

journal homepage: www.elsevier.com/locate/matlet

Predicting and confirming the solidification kinetics for liquid peritectic alloys with large positive mixing enthalpy

Yuhao Wu, Weili Wang, Bingbo Wei *

MOE Key Laboratory of Space Applied Physics and Chemistry, Northwestern Polytechnical University, Xi'an 710072, China

ARTICLE INFO

Article history:
Received 4 May 2016
Received in revised form
21 May 2016
Accepted 24 May 2016
Available online 24 May 2016

Keywords:
Phase separation
Microstructure
Metals and alloys
Phase transformation
Simulation and modeling

ABSTRACT

Those peritectic alloys with large positive mixing enthalpy usually display metastable liquid phase separation. Here, the solidification kinetics for a model $Fe_{50}Cu_{50}$ alloy in broad cooling rate R_c range was predicted by phase-field simulations and confirmed by drop tube experiments. Near-equilibrium peritectic solidification occurs in small R_c regime below 5.62×10^2 K s^{-1}. As R_c rises beyond 7.76×10^2 K s^{-1}, metastable phase separation takes place and results in the formation of a dispersed structure. Afterwards, multilayer core-shell structures appear, and the layer-number varies from two-layer to six-layer with further increasing R_c. Once R_c exceeds 3.64×10^5 K s^{-1}, a dispersed structure once again forms because the core-shell dynamic condition is not satisfied. Non-equilibrium peritectic solidification is induced if R_c is greater than 5.85×10^5 K s^{-1}.

1. Introduction

Metastable liquid phase separation (PS) [1–3] is frequently observed during the solidification of peritectic alloys with large positive mixing enthalpy [4,5]. In recent years, the microstructure evolutions of such alloy systems have been extensively investigated by both experiments [6] and simulations [7]. During rapid solidification, the microstructures of these alloys experience a transition from the peritectic solidification microstructures to the phase separated morphologies with the rise in cooling rate and undercooling [4]. Most of previous investigations related to peritectic alloys with a metastable miscibility gap mainly focused on the microstructure selections in relatively narrow ranges of cooling rate and undercooling [8,9]. So far, the attention to the whole process of microstructure evolution for this kind of alloy is still limited in an ultra-wide cooling rate range.

The phase-field models [10–12] are widely employed to reveal the dynamic processes of elusive microstructure evolution under extreme conditions, such as large undercooling, high cooling rate and strong convection. The high-temperature liquid alloys can be subdivided into numerous droplets with diameters of several tens to hundreds micrometers with drop tube technique [13,14]. This makes it possible to explore the microstructure evolution in cooling rate range from several hundreds to millions Kelvin per second. Selecting a model alloy of $Fe_{50}Cu_{50}$, the aim of this work is to predict the solidification kinetics of liquid peritectic alloy with large positive mixing enthalpy by using a three-dimensional phase-field model, and then provide an experimental confirmation by drop tube method.

2. Methodology

A phase-field model [15,16] was firstly applied to reproduce the evolution processes of metastable phase separation (PS) in tiny droplets of $Fe_{50}Cu_{50}$ alloy. This model considers the liquid phase separation (PS) under the combined effects of Marangoni convection, surface segregation and droplet cooling rate [14]. In this model, the mole concentration C of element Cu is set as the order parameter. The free energy functional of $Fe_{50}Cu_{50}$ alloy droplet can be expressed as

$$F = \int (F_B + F_G + F_S) dV \tag{1}$$

$$F_B = C \cdot g_{Cu} + (1 - C) \cdot g_{Fe} + R_g T_c M C (1 - C) + R_g T \left(C \ln(C) + (1 - C) \ln(1 - C) \right) \tag{2}$$

$$F_G = 0.5 R_g T_c \varepsilon^2 \nabla^2 C \tag{3}$$

$$F_S = R_g T_c \left(\sigma_0 - H_0 C_S + 0.5 g_0 C_S^2 \right) \tag{4}$$

* Corresponding author.
E-mail address: bbwei@nwpu.edu.cn (B. Wei).

http://dx.doi.org/10.1016/j.matlet.2016.05.110
0167-577X/

where F_B is the bulk free energy, F_G is the free energy of concentration gradient, F_S is the surface free energy, R_g is the gas constant, T_c is the critical temperature, T is the temperature, M is the interaction parameter, ε is the characteristic length of spatial heterogeneity, C_S is the surface concentration, g_{Cu} and g_{Fe} are the molar Gibbs free energies of Cu and Fe, σ_0, H_0 and g_0 are the control parameters of surface segregation.

Based on the Model H [14], the dimensionless concentration-field governing equation is derived as

$$\frac{\partial C}{\partial \tau} = \nabla\cdot\left(C(1-C)\nabla\frac{\delta F}{\delta C}\right) - \nabla\cdot(\nu C) + \nabla\cdot\xi \tag{5}$$

where τ is the dimensionless time, ν is the local velocity and ξ is the Gauss noise. To explore the effects of Marangoni convection and cooling rate on the liquid phase separation, a dimensionless heat conduction equation

$$\frac{\partial T_r}{\partial \tau} = \frac{\alpha_T}{D_L}\left(\frac{\partial^2 T_r}{\partial r^2} + \frac{2}{r}\cdot\frac{\partial T_r}{\partial r}\right) \tag{6}$$

is adopted, where T_r is the reduced temperature, α_T and D_L are the thermal and solutal diffusion coefficients. The physical parameters of liquid $Fe_{50}Cu_{50}$ alloy used in calculations are obtained from references [4,17]. The initial and boundary conditions for C and T_r can be found elsewhere [14].

Drop tube experiments of $Fe_{50}Cu_{50}$ alloy were also conducted to confirm the simulation reliability. Each sample had a mass of 3 g and was placed inside a ϕ16 mm × 150 mm quartz tube with a ϕ0.2 mm orifice at its bottom. The quartz tube was then installed on the top of drop tube, which was evacuated to 0.1 MPa in advance and then backfilled with helium gas to 10^5 Pa. The molten alloy melted by induction heating was ejected out from the orifice by high pressure argon gas and dispersed into many droplets, which rapidly solidified during free fall. The solidified microstructures were finally investigated by a Zeiss Axiovert 200 MAT optical microscope and an FEI Sirion 200 scanning electron microscope.

3. Results and discussion

Fig. 1 shows the predicted microstructure morphologies of $Fe_{50}Cu_{50}$ alloy droplets with different cooling rates R_c. Apparently, the simulated microstructures are strongly dependent on R_c. When R_c approaches zero, the driving force of phase separation (PS) is so weak that liquid PS cannot occur, as illustrated in Fig. 1(a-1). In this case, it can be deduced that the near-equilibrium peritectic solidification proceeds based on Fe-Cu phase diagram. As R_c increases beyond 1.04×10^3 K s^{-1}, an unconspicuous PS begins to appear due to the slightly enhanced PS driving force. Although the PS time is relatively long, the volume fraction of Cu-rich liquid is too small to form a core-shell microstructure (CSM) and a dispersed microstructure is formed as seen in Fig. 1(a-2). An evident PS takes place and contributes to the formation of multilayer CSMs assuming that the R_c is greater than1.01×10^3 K s^{-1}, as observed in Fig. 1(b). In such a case, the PS time and the volume fraction of two-coexisting liquids are suitable for core-shell formation (CSF). Moreover, the core-shell layer-number firstly increases and subsequently reduces with the enhancement of R_c. Once R_c exceeds 9.06×10^5 K s^{-1}, it allows little time for the aggregation of two-coexisting liquids before the CSF, and a dispersed structure also forms in Fig. 1(c-1). Provided that the R_c tends to be infinity, the metastable liquid PS is restrained because of the extremely shortened solidification time as given in Fig. 1(c-2), and the non-equilibrium peritectic solidification is activated. It can be concluded that the core-shell formation (CSF) must satisfy two requirements: one is a thermodynamical condition of appropriate volume fractions for two-coexisting liquids, and the other is a dynamical condition of suitable PS time.

When $Fe_{50}Cu_{50}$ alloy is undercooled into the miscibility gap, the homogeneous liquid separates into Fe-rich and Cu-rich liquids. The Cu-rich liquid with a lower surface energy not only migrates to droplet center due to the Marangoni convection, but also flows to droplet surface owing to the surface segregation. This results in the fluctuation of Cu-rich liquid along droplet radial direction and stimulates the formation of multilayer CSM at particular PS times. With PS further continues, the core-shell layer-number gradually decreases so as to lower the system energy, and the CSM becomes more and more stable. The layer-numbers of multilayer CSMs in $Fe_{50}Cu_{50}$ droplets are calculated and the results are given in Fig. 2 (a) and (b). Obviously, the maximum layer-number N_m and the final layer-number N_f during PS are closely related to R_c. With increasing R_c, N_m and N_f increase at first and then decrease, as presented in Figs. 1, 2(a) and (b). In other word, the phase separated morphology transfers from a dispersed structure to a multilayer CSM, and finally evolves into a dispersed structure.

To experimentally verify the theoretical predictions, liquid $Fe_{50}Cu_{50}$ alloy was rapidly solidified inside a drop tube and the solidification microstructures were shown in Fig. 3. According to a heat transfer model [9], the variation of R_c with droplet diameter D can be determined by

$$R_c = 8.08 \times 10^8 \times D^{-1.96}\ K\ s^{-1} \tag{7}$$

At R_c=5.62×10^2 K s^{-1}, the PS driving force is too weak to overcome a barrier of potential energy for phase separation. In this situation, the near-equilibrium peritectic solidification proceeds and the microstructure appears as coarse αFe dendrites dispersed within (Cu) phase, as seen in Fig. 3(a-1). With the rise in R_c, the PS driving force increases and perhaps breaks down the potential

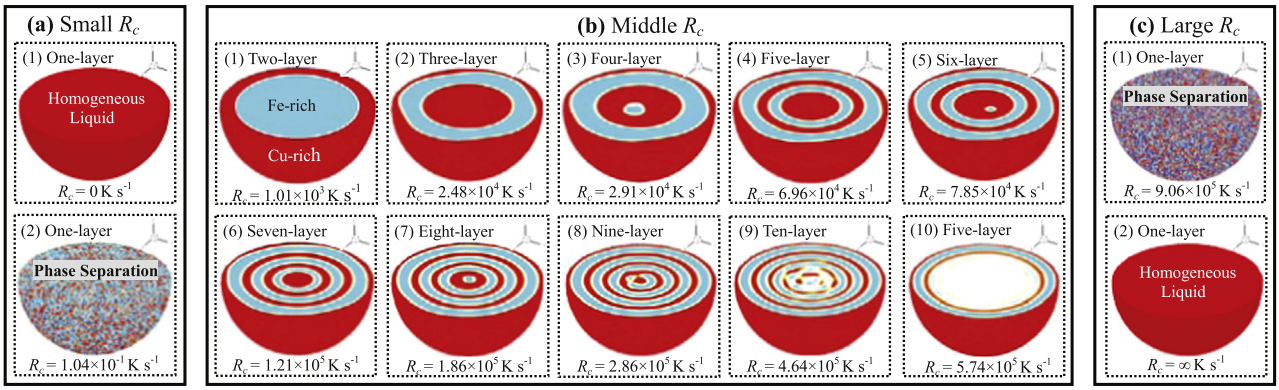

Fig. 1. Predicted microstructure morphologies of $Fe_{50}Cu_{50}$ alloy droplets: (a) small R_c, (b) middle R_c, (c) large R_c.